Miscibility and Multilayer Formation of Fluoroalkane−α,ω-Diol Mixtures at the Air/Water Interface

Takanori Takiue,*,† Fumiya Nakamura,† Hiroyasu Sakamoto,‡ Hiroki Matsubara,† and Makoto Aratono†

Department of Chemistry, Faculty of Sciences, Kyushu University, Fukuoka 812-8581, Japan, and Department of Visual Communication Design, Faculty of Design, Kyushu University, Fukuoka 815-8540, Japan

Received: September 2, 2010; Revised Manuscript Received: November 25, 2010

The surface tension γ of the aqueous solution of 1*H*,1*H*,6*H*,6*H*-perfluorohexane−1,6-diol (FC_6diol) and 1*H*,1*H*,8*H*,8*H*-perfluorooctane−1,8-diol (FC_8diol) mixtures was measured as a function of total molality m and composition of FC_8diol in the mixture X_2 at 293.15 K under atmospheric pressure. The γ vs m curves except at $X_2 = 0$ and 0.05 have a distinct break point due to a phase transition in the adsorbed film. The surface pressure π vs mean area per adsorbed molecule A curves consist of two parts connected by a discontinuous change. The curve was almost vertical just below the phase transition, and the variation of the A value with film composition X_2^H was linear corresponding to the fact that FC_6diol and FC_8diol molecules orient parallel to the surface and are densely packed with the same areas of individual condensed films. Above the phase transition, the A value further decreases to around 0.12−0.19 nm^2 which is much smaller than the cross-sectional area of the fluorocarbon chain, indicating the multilayer formation at the surface. The phase diagram of adsorption (PDA) in the condensed film showed that the m vs film composition X_2^H curve is almost linear and the excess Gibbs energy of adsorption g^{HE}/RT is at most 0.01, manifesting the ideal mixing of molecules. This is in contrast to a positive deviation ($g^{HE}/RT \sim 0.12$) observed in the condensed film of the mixture of 1*H*,1*H*,2*H*,2*H*-perfluorodecanol ($FC_{10}OH$) and 1*H*,1*H*,2*H*,2*H*-perfluorododecanol ($FC_{12}OH$) with perpendicular molecular orientation. The loss of dispersion interaction between different species having different chain lengths is more appreciable in the perpendicular condensed films and thus leads to less miscibility of $FC_{10}OH$ and $FC_{12}OH$. In the parallel condensed film, on the other hand, FC_6diol and FC_8diol molecules can arrange their position as close as possible to minimize the loss of dispersion interaction. The X_2^H value in the multilayer is close to unity, and thus, the multilayer consists of almost FC_8diol molecules which form a multilayer in the single-component system. Furthermore, the condensed monolayer−multilayer phase transition was accompanied by a large increase in surface density of FC_8diol and a small decrease in that of FC_6diol, indicating that FC_8diol molecules pile preferentially to form a multilayer.

Introduction

The adsorption of mixed component systems at soft interfaces such as gas/liquid and liquid/liquid interfaces is of great importance and interest in the field of technology as well as in basic science, and hence, many workers have explored it experimentally and theoretically.[1,2] Since the structure and property of adsorbed films of mixtures are essentially governed not only by the adsorption characteristics of individual components but also the mutual interaction between them in the adsorbed films, studies on the mutual interaction in the mixed adsorbed films are indispensable to understand the structure−function relation of complicated molecular organized systems, such as emulsions, vesicles, and biological membranes. We have investigated the mixed adsorption of various surface-active substances at soft interfaces on the basis of interfacial tension measurements and reliable thermodynamic data analysis. One of our outstanding methods is that the miscibility of molecules in the adsorbed film was elucidated quantitatively by constructing the phase diagram of adsorption (PDA) and evaluating the excess thermodynamic quantity of adsorption.[3]

Recently, the adsorption behavior of 1*H*,1*H*,8*H*,8*H*-perfluorooctane−1,8-diol (FC_8diol) at the aqueous solution/air interface has been studied in order to clarify the effects of the rigidity of the fluorocarbon (FC) chain and two terminal hydroxyl groups on the adsorbed film from the viewpoints of entropy and energy of adsorption.[4] One of the important findings is that FC_8diol forms a condensed monolayer with parallel molecular orientation, which is striking contrast to the "wicket-like" conformation of Bolaform surfactants with the flexible hydrocarbon (HC) chain at the aqueous solution/air interface.[5−7] Another noticeable point is that the molecules pile spontaneously to form a multilayer at high concentrations and low temperatures, and the FCdiol molecules are packed more densely in the multilayer at the aqueous solution/air interface than at the hexane solution/water interface because of the fact that hexane molecules intercalate into the upper layer of the multilayer.[8,9] Furthermore, the positive entropy change of adsorption observed at the aqueous solution/air interface is attributable to the dehydration around the hydrophobic chain accompanied by the adsorption.[4]

In our previous study on the adsorption of a homologous FC alcohol mixture with the different chain length by only two, such as 1*H*,1*H*,2*H*,2*H*-perfluorodecanol ($FC_{10}OH$) and 1*H*,1*H*,2*H*,2*H*-perfluorododecanol ($FC_{12}OH$), at the hexane solution/water interface, the miscibility of both alcohols in the adsorbed film

* To whom correspondence should be addressed. Phone: +81 92 642 2578. Fax: +81 92 642 2607. E-mail: t.takiue@chem.kyushu-univ.jp.
† Department of Chemistry.
‡ Department of Visual Communication Design.

10.1021/jp1083696
Published on Web 12/30/2010

was examined by constructing the PDA and evaluating the excess Gibbs energy of adsorption $g^{H,E}$.[10] It was shown that the mixing of $FC_{10}OH$ and $FC_{12}OH$ is almost ideal in the gaseous and expanded states, while it is nonideal and accompanies a positive $g^{H,E}$ value in the condensed state. Taking account of the experimental findings obtained by X-ray reflectivity measurements that both FC alcohols stand almost perpendicularly at the interface in the condensed film,[11,12] these results were reasonably explained by the fact that the loss of dispersion interaction between hydrophobic chains due to the chain length mismatch appreciably affects the miscibility of molecules in the condensed state.

The effect of molecular orientation on the miscibility of molecules in the adsorbed film was studied recently on the mixture of 1*H*,1*H*,10*H*,10*H*-perfluorodecane−1,10-diol (FC_{10}diol) with parallel orientation and $FC_{12}OH$ with normal one at the hexane solution/water interface.[13] The mixture exhibited three kinds of film states—parallel condensed, normal condensed, and multilayer states—depending on the concentration and bulk composition. The PDA suggested that the micro phase separation takes place due to the mismatch of the molecular orientation in the parallel condensed monolayer, and that FC_{10}diol molecules may stand upright and mix with $FC_{12}OH$ molecules in the normal condensed monolayer. Furthermore, the multilayer is much richer in FC_{10}diol than in $FC_{12}OH$ when the multilayer is evolved from the parallel condensed monolayer, while the fraction of $FC_{12}OH$ increases rapidly when it is evolved from the normal condensed monolayer, suggesting that the structure changes drastically with film composition.

Our next interest is to know the effect of parallel orientation on the mixing of molecules in the adsorbed film. In this study, therefore, we employed the mixture of FC_8diol and its homologue, 1*H*,1*H*,6*H*,6*H*-perfluorohexane−1,6-diol (FC_6diol) and investigated the adsorbed film of their mixture at the aqueous solution/air interface. Since FC_8diol forms a condensed monolayer with parallel molecular orientation, FC_6diol may also form it as FC_8diol. Even when FC_6diol does not form it, however, it is highly valuable to clarify how FC_6diol influences the formation of the multilayer of FC_8diol.

Experimental Section

Materials. FC_8diol and 1*H*,1*H*,6*H*,6*H*-perfluorohexane−1,6-diol (FC_6diol) were employed as solutes. The purification procedure of FC_8diol was described elsewhere.[4] FC_6diol purchased from Tokyo Chemical Industry Co, Ltd., was purified by recrystallization once from chloroform solution. Its purity was checked by observing no time dependence of equilibrium surface tension of the aqueous solution and by liquid−gas chromatography.

Surface Tensiometry. The surface tension γ of the aqueous solution of FC_6diol and FC_8diol mixtures was measured as a function of total molality m and bulk composition of FC_8diol X_2 at 293.15 K under atmospheric pressure by the pendant drop method.[14] Here, m and X_2 are defined, respectively, by

$$m = m_1 + m_2 \quad (1)$$

and

$$X_2 = m_2/m \quad (2)$$

where m_1 and m_2 are the molalities of FC_6diol and FC_8diol, respectively. For the calculation of surface tension, the difference in the densities of air and pure water were used instead of those of air and the aqueous solution, because the concentration was sufficiently low. The experimental error of the γ value was estimated within ± 0.05 mN m^{-1}.

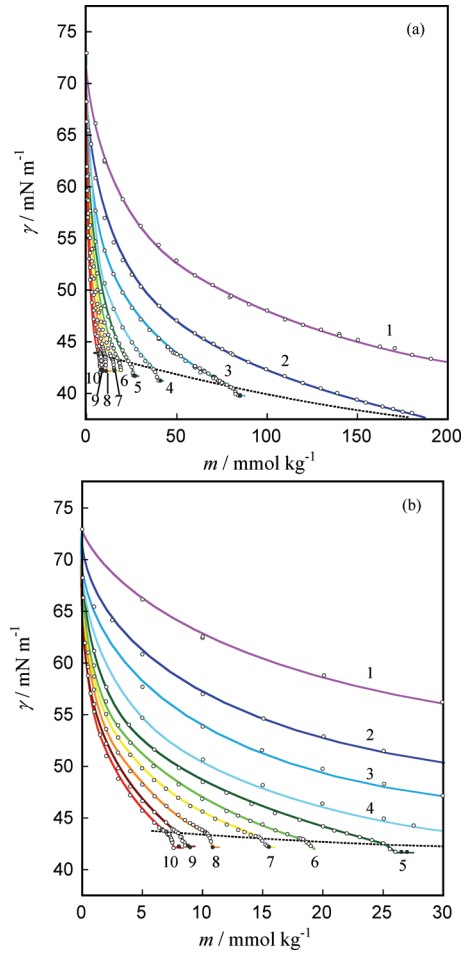

Figure 1. Surface tension vs total molality curves at constant composition: X_2 = (1) 0 (FC_6diol), (2) 0.05, (3) 0.1, (4) 0.2, (5) 0.3, (6) 0.4, (7) 0.5, (8) 0.7, (9) 0.9, (10) 1 (FC_8diol).

Results and Discussion

Figure 1a shows the surface tension γ of the aqueous solution of FC_6diol and FC_8diol mixture vs total molality m curves at given bulk compositions X_2 at 293.15 K under atmospheric pressure. The curves at low concentrations are magnified in Figure 1b. The γ value decreases gradually with increasing m. The curves except at $X_2 = 0$ (pure FC_6diol) and 0.05 have a break point due to the phase transition in the adsorbed film. Above the break points, the γ value decreases very steeply with a small increase in m. The surface tension γ^{eq} and the total molality m^{eq} at the break point are plotted against X_2 in Figures 2 and 3. The γ^{eq} value increases and the corresponding m^{eq} decreases with increasing X_2. It is noted that the other break point was observed on the γ vs m curve at higher concentration m^s, above which the γ value is almost independent of m, as shown by filled circles. Since a tiny deposit was found in the aqueous solution above m^s, m^s is regarded as the solubility of solutes in water. We will refer to this later.

Here, we briefly mention the thermodynamic equations for analyzing the experimental results. Since the solutes in this study are both nonionic, the total differential of surface tension γ is

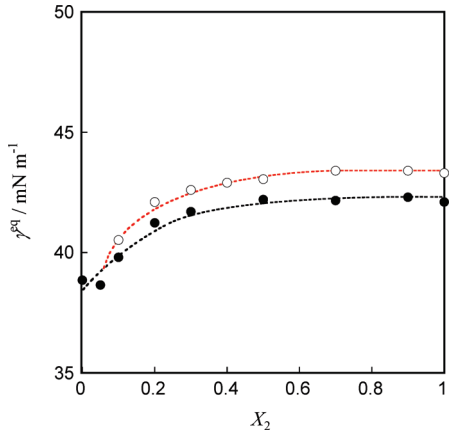

Figure 2. Equilibrium surface tension vs composition curves: (○) γ^{eq} vs X_2; (●) γ^S vs X_2.

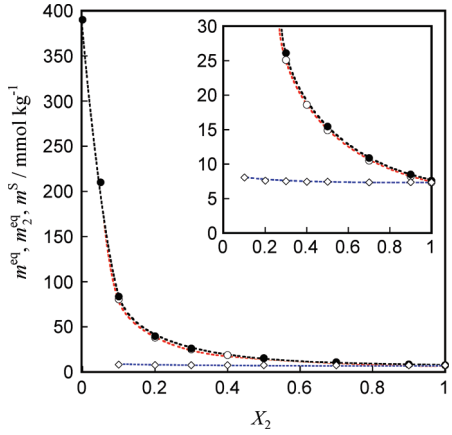

Figure 3. Equilibrium total molality vs composition curves: (○) m^{eq} vs X_2; (◇) m_2^{eq} vs X_2; (●) m^S vs X_2. The low concentration range is enlarged in the inset.

expressed as a function of temperature T, pressure p, and chemical potential of component i, μ_i (i = 1, 2), by

$$d\gamma = -s^H dT + v^H dp - \Gamma_1^H d\mu_1 - \Gamma_2^H d\mu_2 \qquad (3)$$

where s^H, v^H, and Γ_i^H are, respectively, the surface excess entropy, volume, and the number of moles of component i per unit area defined with reference to the two dividing planes making the excess numbers of moles of air and water zero, simultaneously.[15] Assuming the aqueous solution to be ideally dilute and substituting the total differential of chemical potential into eq 3, we have

$$d\gamma = -\Delta s dT + \Delta v dp - \Gamma^H(RT/m)dm - \Gamma^H(RT/X_1X_2)(X_2^H - X_2)dX_2 \qquad (4)$$

where Δs and Δv are, respectively, the entropy and volume associated with adsorption, Γ^H the total surface density of FC_6diol and FC_8diol, and X_2^H the composition of FC_8diol in the adsorbed film. They are, respectively, defined by

$$\Delta y = y^H - \Gamma_1^H y_1^W - \Gamma_2^H y_2^W \qquad y = s, v \qquad (5)$$

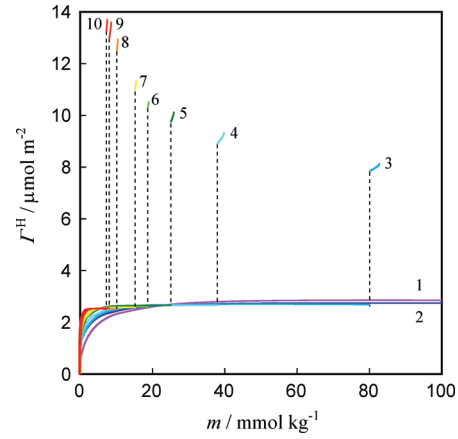

Figure 4. Total surface density vs total molality curves at constant composition: X_2 = (1) 0 (FC_6diol), (2) 0.05, (3) 0.1, (4) 0.2, (5) 0.3, (6) 0.4, (7) 0.5, (8) 0.7, (9) 0.9, (10) 1 (FC_8diol).

$$\Gamma^H = \Gamma_1^H + \Gamma_2^H \qquad (6)$$

and

$$X_2^H = \Gamma_2^H/\Gamma^H \qquad (7)$$

In order to characterize the state of the adsorbed films, first, the total surface density Γ^H was calculated by applying the equation

$$\Gamma^H = -(m/RT)(\partial\gamma/\partial m)_{T,p,X_2} \qquad (8)$$

to the γ vs m curves in Figure 1. The results are shown as the Γ^H vs m curves in Figure 4. The Γ^H value increases with increasing m and becomes almost constant around 2.5−3.0 μmol m^{-2} just below the phase transition point. Furthermore, the values are around 8−13 μmol m^{-2} just above the phase transition. It should be noted that 8−13 μmol m^{-2} is much larger than the surface density of around 6 μmol m^{-2} expected for the condensed monolayer, where FC_8diol molecules are densely packed with the molecular orientation perpendicular to the surface.

The surface pressure π vs mean area per adsorbed molecule A curves are constructed by using the following equations

$$\pi = \gamma^0 - \gamma \qquad (9)$$

and

$$A = 1/N_A\Gamma^H \qquad (10)$$

where γ^0 is the surface tension of the pure water and N_A is Avogadro's number. The π vs A curves at constant X_2 are drawn in Figure 5. The curve of pure FC_8diol (curve 10) consists of two parts connected by a discontinuous change; the two states were assigned to be the monolayer and multilayer. Especially the π value increases very sharply with a small decrease in A, and A is 0.66 nm^2 just below the phase transition, indicating that FC_8diol molecules are densely packed with parallel molecular orientation (parallel condensed state). In the case of the pure FC_6diol system (curve 1), the π value increases gradually

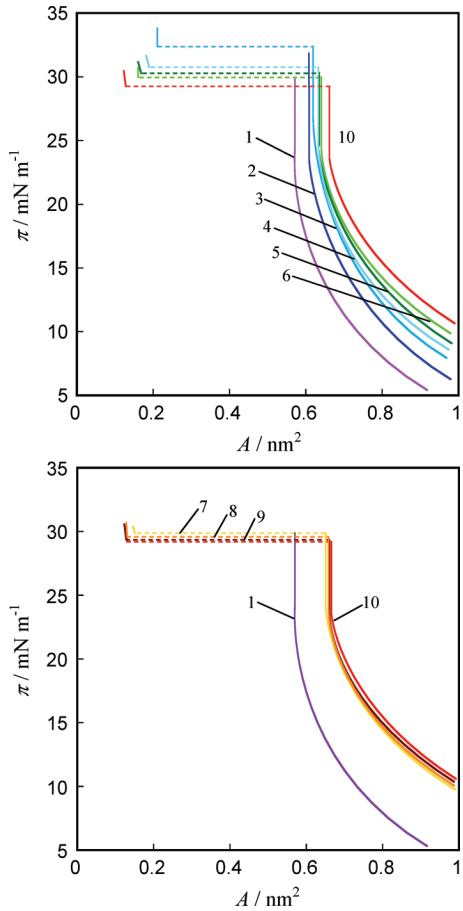

Figure 5. Surface pressure vs mean area per adsorbed molecule curves at constant composition: (a) $X_2 = 0$ (FC_6diol), (2) 0.05, (3) 0.1, (4) 0.2, (5) 0.3, (6) 0.4, (10) 1 (FC_8diol); (b) $X_2 = 0$ (FC_6diol), (7) 0.5, (8) 0.7, (9) 0.9, (10) 1 (FC_8diol).

with decreasing A at lower surface pressures and rises almost vertically at higher ones. The minimum A value is about 0.57 nm^2 which is very close to the calculated cross-sectional area (0.56 nm^2) along the major axis of FC_6diol, and therefore, it is concluded that FC_6diol molecules form a parallel condensed monolayer at the surface.

Figure 5 also represents two essential differences in the film states between the pure systems. One is that the A value in the parallel condensed monolayer is smaller for FC_6diol than for FC_8diol because of the shorter FC chain length of FC_6diol than that of FC_8diol. The other is that, although FC_8diol molecules pile spontaneously to form a multilayer at high concentrations, FC_6diol ones do not form it even at the highest concentrations close to the solubility in the water phase. This may be mainly due to the weaker dispersion interaction between FC_6diol molecules than between FC_8diol ones.

In the mixed system, the π vs A curves consist of two parts connected by a discontinuous change. Below the phase transition, the A values at given π change regularly from the value of pure FC_6diol to that of pure FC_8diol with increasing X_2, suggesting that both components are mixed in the adsorbed film. The π value increases very steeply with a small decrease in A just below the phase transition, which indicates extremely low compressibility of the adsorbed film like two-dimensional solid state. In Figure 6 are plotted the A values at $\pi = 27.9$ mN m^{-1} ($\gamma = 45$ mN m^{-1}), which is just below the transition pressure π^{eq}, against film composition X_2^H. The solid line represents the variation of A with X_2^H corresponding to that FC_6diol and FC_8diol molecules orient parallel to the surface and are densely packed

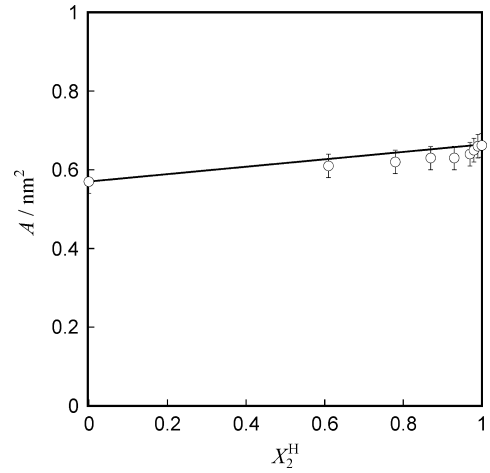

Figure 6. Mean area per adsorbed molecule vs film composition plots at $\gamma = 45$ mN m^{-1}.

with the same areas of their individual condensed films ($A_1^0 = 0.57$ nm^2 for FC_6diol and $A_2^0 = 0.66$ nm^2 for FC_8diol), given by

$$A = A_1^0 X_1^H + A_2^0 X_2^H \tag{11}$$

The plots are very close to the line within experimental error, and thus, it is manifested that FC_6diol and FC_8diol molecules are keeping their parallel molecular orientation of the respective condensed states and mixed with each other. Above the phase transition, on the other hand, the A values further decrease to around 0.12−0.19 nm^2. This is much smaller than the cross-sectional area of the FC chain (0.28 nm^2), and thus, the film state was assigned to be a multilayer. Furthermore, it is noted that π^{eq} increases with decreasing X_2; multilayer formation is certainly affected by addition of FC_6diol into FC_8diol.

In order to examine the mixing of FC_6diol and FC_8diol in both monolayers and multilayers, it is highly advantageous to estimate the composition of adsorbed film X_2^H. The X_2^H values were estimated by applying the following equation[3]

$$X_2^H = X_2 - (X_1 X_2/m)(\partial m/\partial X_2)_{T,p,\gamma} \tag{12}$$

to the m vs X_2 curves (solid lines) in Figure 7, and then, the combination of the m vs X_2^H curve (broken lines) with the m vs X_2 curve at a given surface tension forms the phase diagram of adsorption (PDA).

Figure 7a shows the PDA of monolayers with relatively low surface densities. The m vs X_2^H curve only slightly deviates from the straight dotted line representing the ideal mixing of components in the adsorbed film given by[3]

$$m = m_1^0 + (m_2^0 - m_1^0)X_2^H \tag{13}$$

Essentially, the same feature was realized at 45 mN m^{-1} just below the phase transition point (parallel condensed monolayer), as shown in Figure 7b. These results indicate that the mixing of FC_6diol and FC_8diol is almost ideal in the adsorbed monolayer.

The miscibility of FC_6diol and FC_8diol in the monolayer state can be discussed more quantitatively by evaluating the excess Gibbs energy of adsorption $g^{H,E}$ given by

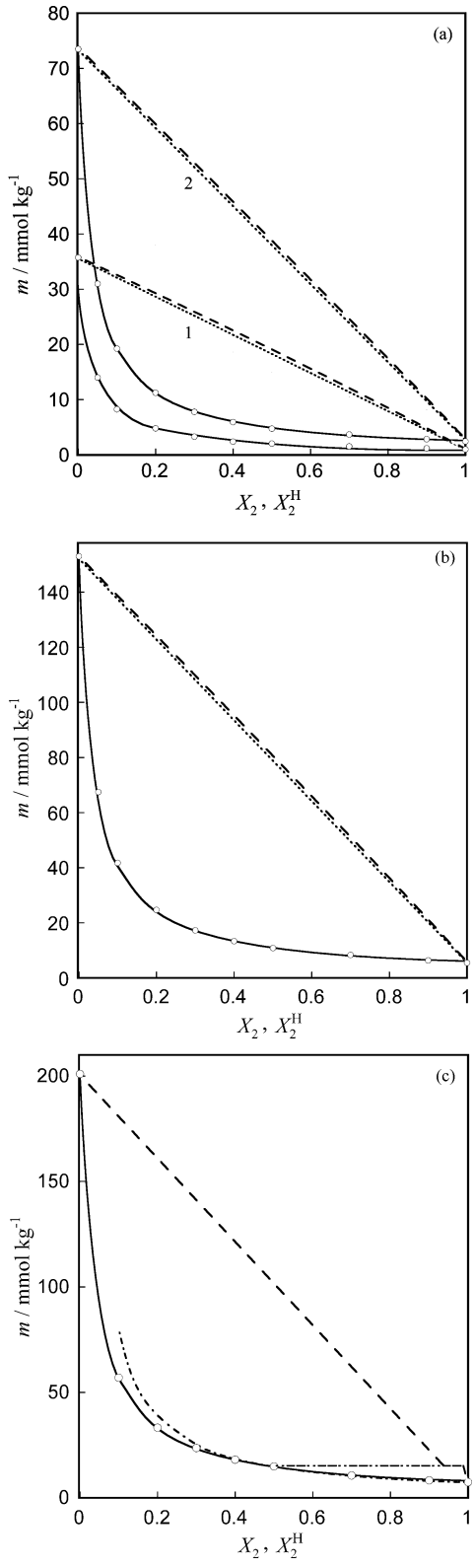

Figure 7. Total molality vs composition curves at constant surface tension: (a) γ = (1) 55, (2) 50 mN m^{-1}; (b) γ = 45 mN m^{-1}; (c) γ = 43 mN m^{-1}; (—) m vs X_2; (– – –) m vs X_2^H; (•••) ideal mixing line given by eq 13; (– • –) m^{eq} vs X_2.

$$g^{H,E} = RT(X_1^H \ln f_1^H + X_2^H \ln f_2^H) \qquad (14)$$

where f_i^H is the activity coefficient of component i in the adsorbed film defined symmetrically as $f_i^H \rightarrow 1$ when $X_i^H \rightarrow 1$, and calculated by

$$f_i^H = X_i m / X_i^H m_i^0 \qquad i = 1, 2 \qquad (15)$$

Making use of these equations and PDA in Figure 7a and b, we obtained $g^{H,E}$ values at given γ values. The results are shown as $g^{H,E}$ vs X_2^H curves at γ = 55, 50, and 45 mN m^{-1} in Figure 8. The $g^{H,E}$ value is slightly positive at all film compositions and almost independent of γ within error. This indicates that the excess area per adsorbed molecule is almost zero, which is consistent with the linear variation of A with X_2^H in Figure 6.[16]

The effect of molecular orientation on the miscibility of molecules in the adsorbed films is well understood by comparing the $g^{H,E}$ values with those for the mixed systems of homologous FC alcohols with normal molecular orientation. In our previous study on the miscibility of 1*H*,1*H*,2*H*,2*H*-perfluorodecanol ($FC_{10}OH$) and 1*H*,1*H*,2*H*,2*H*-perfluorododecanol ($FC_{12}OH$) at the hexane/water interface, we found that both alcohols orient almost perpendicularly and mix ideally in the gaseous and expanded states and nonideally in the condensed state even though their difference of chain length is only two.[10] Thus, the difference in molecular orientation is probably more influential on the condensed films than on the gaseous and expanded states. In Figure 9, the $g^{H,E}/RT$ vs X_2^H curve in the parallel condensed monolayer at γ = 45 mN m^{-1} of the mixed FC_6diol−FC_8diol system is shown together with that in the normal condensed monolayer at γ = 40 mN m^{-1} of the mixed $FC_{10}OH$−$FC_{12}OH$ system. The value of the former is at most 0.013 ($g^{H,E}$ ∼0.03 kJ mol^{-1}) and much smaller than that of the latter, ca. 0.12 ($g^{H,E}$ ∼0.3 kJ mol^{-1}). It is said that the loss of dispersion interaction between the different species having different chain lengths is more appreciable in the perpendicular condensed films and thus leads to less miscibility of $FC_{10}OH$ and $FC_{12}OH$. In the parallel condensed films, on the other hand, the FC_6diol and FC_8diol molecules can arrange their positions as close as possible to minimize the loss of dispersion interaction.

Now let us examine the miscibility in the multilayer. In Figure 7c is shown the PDA at γ = 43 mN m^{-1} at which the adsorbed film is in a multilayer state above and a condensed monolayer state below X_2 = 0.5. The m vs X_2^H curve is almost linear in the condensed monolayer as discussed above. It should be noted that the X_2^H value is larger in the multilayer than in the condensed monolayer and close to unity at the phase transition point. Therefore, it is said that the multilayer consists of almost all FC_8diol molecules, which form a multilayer in the single-component system.

In Figure 3, the m_2^{eq} vs X_2 curve is shown together with the m^{eq} vs X_2 curve at the monolayer−multilayer phase transition point. The curves at low concentrations are magnified in the inset. The m_2^{eq} value increases slightly with decreasing X_2; the addition of FC_6diol influences the transition. The effect of the addition of FC_6diol on the formation of multilayer is clearly seen by referring to Figures 2 and 3; the former displays m^s at the saturation concentration and m^{eq} at the condensed monolayer−multilayer transition point as a function of X_2 and the latter does the corresponding surface tension γ^s and γ^{eq} vs X_2 curves. The m^s value increases and the γ^s value decreases with decreasing X_2. The point is that the multilayer region between m^{eq} and m^s and, thus, the one between γ^{eq} and γ^s becomes narrower with decreasing X_2 and eventually disappears below X_2 = 0.06, suggesting that an addition of FC_6diol prevents the formation of multilayer.

Finally, let us briefly mention an expected structure of multilayer found in this study. At the condensed monolayer−multilayer transition, the following equation holds:[19]

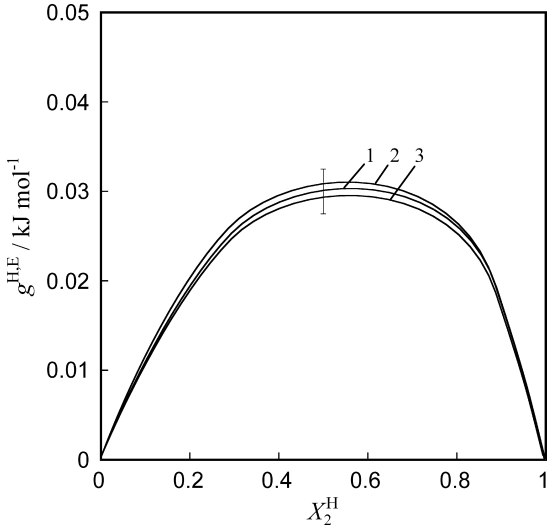

Figure 8. Excess Gibbs energy of adsorption vs film composition curves at constant surface tension: γ = (1) 55, (2) 50, (3) 45 mN m^{-1}.

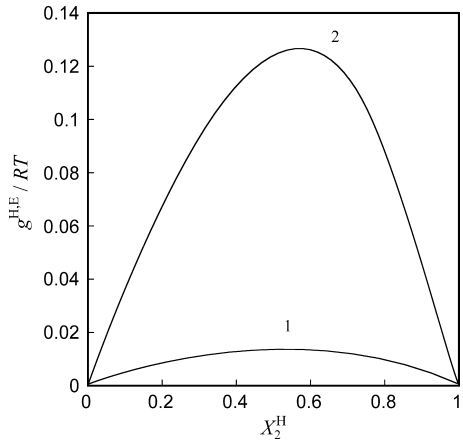

Figure 9. Excess Gibbs energy of adsorption vs film composition curves in the condensed state: (1) FC_6diol−FC_8diol mixture at γ = 45 mN m^{-1}, (2) FC_{10}OH−FC_{12}OH mixture at γ = 40 mN m^{-1}.

$$X_2^{H,M} - X_2^{H,C} = -(X_1X_2/RT)(1/\Gamma^{H,M} - 1/\Gamma^{H,C})(\partial\gamma^{eq}/\partial X_2)_{T,p} \quad (16)$$

where $X_2^{H,M}$ and $X_2^{H,C}$ are, respectively, the composition of multilayer and condensed monolayer at the transition point. By using the γ^{eq} vs X_2 curve and Γ^H values at the phase transition point, the $X_2^{H,M} - X_2^{H,C}$ values were estimated and plotted against X_2 in Figure 10. Taking note of that the $X_2^{H,C}$ values at the condensed monolayer−multilayer transition points are expected to those given in Figure 7b because the PDA is constructed at very close to the phase transition points, and also employing the results given in Figure 10, we have $X_2^{H,M} \approx 1$ at all X_2. This demonstrates that FC_8diol molecules preferentially pile on the first layer, which is expected to be akin to the condensed monolayer being in equilibrium with the multilayer at the phase transition point. This is in accord with the findings that FC_6diol does not but FC_8diol does form the multilayer. The multilayer may not be homogeneous but heterogeneous in thickness judging from a continuous increase in $\Gamma^{H,M}$. X-ray reflectivity measurement will provide definite information about the multilayer structure at the microscopic scale.[17,18]

The preferential piling of FC_8diol molecules was further examined by evaluating the ratio of the change in surface densities of individual components at the condensed monolayer−multilayer phase transition, $\Delta\Gamma_1^H/\Delta\Gamma_2^H = (\Gamma_1^{H,M} - \Gamma_1^{H,C})/(\Gamma_2^{H,M} - \Gamma_2^{H,C})$. Employing the expression for γ as a function of m_2 and X_2 at constant T and p given by

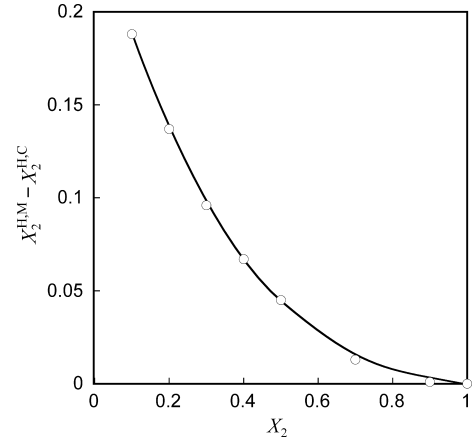

Figure 10. Change in film composition vs composition curve at condensed monolayer−multilayer transition.

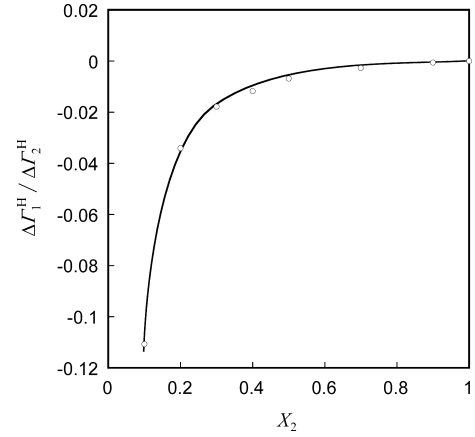

Figure 11. Ratio of changes in surface densities of FCdiol at condensed monolayer−multilayer transition vs composition curve.

$$d\gamma = -\Gamma^H(RT/m_2)dm_2 + \Gamma_1^H(RT/X_1X_2)dX_2 \quad (17)$$

and eliminating $d\gamma^{eq}$ from the equations at the transition points, we have

$$\frac{\Delta\Gamma_1^H}{\Delta\Gamma_2^H} = \frac{X_1(\partial m_2^{eq}/\partial X_2)_{T,p}}{m^{eq} - X_1(\partial m_2^{eq}/\partial X_2)_{T,p}} \quad (18)$$

Thus, the values were calculated by applying eq 18 to the m_2^{eq} vs X_2 curve in Figure 3, and plotted against X_2 in Figure 11. The value is negative and its absolute one is much smaller than unity, indicating that Γ_2^H increases very largely while Γ_1^H decreases slightly at the phase transition point ($\Gamma_2^{H,C}$ = 2.42, $\Gamma_2^{H,M}$ = 10.89, $\Gamma_1^{H,C}$ = 0.15, and $\Gamma_1^{H,M}$ = 0.11 μmol m^{-2} at X_2 = 0.5). This clearly demonstrates that FC_8diol molecules pile preferentially to form a multilayer.

Acknowledgment. This work was supported in part by the *Grant-in-Aid for Scientific Research on Innovative Areas* (Soft Interface Science) of the Ministry of Education, Culture, Sports, Science and Technology of Japan (No. 21106515).

References and Notes

(1) Holland, P. M.; Rubingh, D. N. *Mixed Surfactant Systems*; ACS Symposium Series 501; American Chemical Society: Washington, DC, 1992.

(2) Abe, M.; Scamehorn, J. F. *Mixed Surfactant Systems*; Surfactant Science Series 124; Dekker: New York, 2005.

(3) Aratono, M.; Villeneuve, M.; Takiue, T.; Ikeda, N.; Iyota, H. *J. Colloid Interface Sci.* **1998**, *200*, 161.

(4) Takiue, T.; Nakamura, F.; Murakami, D.; Fukuda, T.; Shuto, A.; Matsubara, H.; Aratono, M. *J. Phys. Chem. B* **2009**, *113*, 6305.

(5) Menger, F. M.; Wrenn, S. *J. Phys. Chem.* **1974**, *78*, 1387.

(6) Abid, S. K.; Hamid, S. M.; Sherrington, D. C. *J. Colloid Interface Sci.* **1987**, *120*, 245.

(7) Aspée, A.; Lissi, E. A. *J. Colloid Interface Sci.* **1998**, *205*, 482.

(8) Takiue, T.; Fukuda, T.; Murakami, D.; Inomata, H.; Sakamoto, H.; Matsubara, H.; Aratono, M. *J. Phys. Chem. C* **2008**, *112*, 5078.

(9) Takiue, T.; Fukuda, T.; Murakami, D.; Sakamoto, H.; Matsubara, H.; Aratono, M. *J. Phys. Chem. B* **2009**, *113*, 14667.

(10) Takiue, T.; Fukuta, T.; Matsubara, H.; Ikeda, N.; Aratono, M. *J. Phys. Chem. B* **2001**, *105*, 789.

(11) Zhang, Z.; Mitrinovic, D. M.; Williams, S. M.; Huang, Z.; Schlossman, M. L. *J. Chem. Phys.* **1999**, *110*, 7421.

(12) Pingali, S. V.; Takiue, T.; Luo, G.; Tikhonov, A. M.; Ikeda, N.; Aratono, M.; Schlossman, M. L. *J. Phys. Chem. B* **2005**, *109*, 1210.

(13) Murakami, D.; Fukuda, T.; Matsubara, H.; Aratono, M.; Takiue, T. *Colloids Surf., A* **2010**, *354*, 205.

(14) Sakamoto, H.; Murao, A.; Hayami, Y. *J. Inst. Image Inf. Television Eng.* **2002**, *56*, 1643.

(15) Motomura, K. *J. Colloid Interface Sci.* **1978**, *64*, 348.

(16) Takiue, T.; Matsuo, T.; Ikeda, N.; Motomura, K.; Aratono, M. *J. Phys. Chem. B* **1998**, *102*, 5840.

(17) Schlossman, M. L. *Curr. Opin. Colloid Interface Sci.* **2002**, *7*, 235.

(18) Yano, Y. F.; Uruga, T.; Tanida, H.; Toyokawa, H.; Terada, Y.; Takagaki, M.; Yamada, H. *Langmuir* **2009**, *25*, 32.

(19) Shibata, K.; Matsuda, T.; Fujimoto, R.; Matsubara, H.; Takiue, T.; Aratono, M. *Colloids Surf., A* **2004**, *250*, 443.

JP1083696